Journal of Molecular Catalysis A: Chemical 303 (2009) 141–147

Contents lists available at ScienceDirect

Journal of Molecular Catalysis A: Chemical

journal homepage: www.elsevier.com/locate/molcata

Favorable recycling photocatalyst TiO_2/CFA: Effects of loading method on the structural property and photocatalytic activity

Jian-wen Shi*, Shao-hua Chen*, Shu-mei Wang, Peng Wu, Gui-hua Xu

Key Laboratory of Urban Environment and Health, Institute of Urban Environment, No. 1799, Ji-Mei-Da-Dao, Chinese Academy of Sciences, Xiamen, Fujian, 361021, China

ARTICLE INFO

Article history:
Received 21 October 2008
Received in revised form
23 December 2008
Accepted 12 January 2009
Available online 20 January 2009

Keywords:
Titanium dioxide
Coal fly ash
Immobilization
Photocatalytic activity

ABSTRACT

In order to more easily separate TiO_2 photocatalyst from the treated wastewater, TiO_2 was immobilized on the surface of coal fly ash by employing three kinds of approaches, sol–gel procedure, ambient hydrolysis procedure and hybrid slurry procedure. The effects of loading method on the structural property of TiO_2-coated coal fly ash (TiO_2/CFA), such as morphology, crystal structure, porous property and ultraviolet-visible absorption were investigated, and the photocatalytic activity of TiO_2/CFA was evaluated by the photocatalytic depigmentation and mineralization of methyl orange solution. The results show that TiO_2/CFA particles are easy to precipitate and recover from water. The hybrid slurry procedure is a more proper method to immobilize TiO_2 on coal fly ash than the other two procedures because the TiO_2/CFA sample prepared by hybrid slurry procedure exhibits higher photocatalytic activity and better repeatability.

1. Introduction

The environmental pollution is increasing in recent decades due to rapid industrialization and population growth throughout the world [1,2]. Water quality is continuously deteriorating due to addition of toxic as well as colored effluents from textile, paper, carpet, leather, distillery and printing industries, pharmaceutical plants [2–6]. Many technologies, including physical, chemical, and biological methods, have been developed to deal with environment pollution [7–10]. Among them, the photocatalytic oxidation process using heterogeneous photocatalysis is regarded as a promising technology to decompose harmful pollutants to final non-toxic products [11–13]. Titanium dioxide in anatase form has attracted much interest of many researchers because of its high stability, nontoxicity and inexpensiveness [14–16]. In the past decade, the TiO_2-photocatalytic degradation of organic pollutants under UV irradiation has proven to be a very effective process, which could accelerate the complete mineralization of organic pollutants [17–20]. However, one of the main problems limited the practical applications of TiO_2 to water treatment so far is that the suspended TiO_2 particles are very difficult to separate and recover from water because of their small particle size [21–23].

This problem can be solved, in part, if TiO_2 is immobilized on some substrates without the loss of activity [24–28]. Silica, zeolite, alumina, activated carbon, and activated carbon fibers have been used as substrates by some researchers for TiO_2 immobilization in the removal of the pollutants from water [8,29–32]. Among them, activated carbon is most commonly used as substrate for TiO_2 immobilization due to its porous structure and adsorption property [33,34]. But activated carbon is a costly material, which will increase the cost of water treatment.

Coal fly ash (CFA) is one of the solid wastes largely produced from power generation. It is well known that CFA is a valuable and desirable additive to cement concrete because of its spherical shape and pozzolanic properties [35,36]. Currently, its applications are only limited to civil engineering including cement and brick production and as a filling in road work [37]. The rate of increase in demand in these applications is far less than the rate of increase in production. There are growing concerns about CFA disposal problems. Therefore, research is needed to develop new alternative environmental friendly applications that can further exploit CFA.

Immobilizing TiO_2 on the surface of CFA, and then using the prepared material as photocatalyst for the treatment of organic compounds in water, may be a good attempt to solve these problems described above. CFA particles are easy to precipitate in water because of their larger particle size and heavier weight comparing with nanometer TiO_2 particles, so the separateness and recovery of catalyst from water will be realized when TiO_2 is immobilized on CFA. At the same time, a new application of CFA will be developed. However, the investigations immobilizing TiO_2 on the surface of CFA have seldom been reported. To the best of our knowledge, only two reports mentioning the immobilization of TiO_2 on CFA can be found in the literature [38,39]. Yu [38] immobilized TiO_2 on CFA by a precipitation method using $TiCl_4$ and NH_4HCO_3 as the reaction

* Corresponding author. Tel.: +86 592 6190529 fax: +86 592 6190977.
E-mail addresses: shijnwn@163.com (J.-w. Shi), shchen@iue.ac.cn (S.-h. Chen).

1381-1169/$ – see front matter © 2009 Elsevier B.V. All rights reserved.
doi:10.1016/j.molcata.2009.01.016

reagent, and studied the photocatalytic property of the prepared material by the removal test of NO gas, but the recycling property of TiO_2/CFA had not been investigated. Shin et al. [39] also prepared TiO_2-coated CFA by the same method (precipitation method), and they researched the influences of pH of the solution, the addition rate of NH_4HCO_3 and the stirring speed of magnetic stirrer on the photocatalytic property of TiO_2/CFA by the decomposition of acetic acid. However, the recycling property of TiO_2/CFA had not been researched, either.

Although TiO_2 have been immobilized on the surface of CFA successfully by Yu [38] and Shin et al. [39] in previous work, several questions remain unclear: (1) is the precipitation method necessary, or is it possible to immobilize TiO_2 on CFA by a more simple method? (2) Is the photocatalyst TiO_2/CFA easy to separate from the treated wastewater? (3) What is the recycling property of TiO_2/CFA? The objective of the current work is not only to clarify these important issues, but also to explore the effects of loading method on the structural property and photocatalytic activity of TiO_2/CFA. We immobilized TiO_2 on the surface of CFA by using three methods, sol–gel procedure, ambient hydrolysis procedure and hybrid slurry procedure, respectively. Sol–gel is a versatile technique of metal oxides preparation and has been used widely to load TiO_2 on some substrates [40–42], but we have not found that sol–gel procedure was utilized to load TiO_2 on CFA. Moreover, as far as we know that the ambient hydrolysis procedure and hybrid slurry procedure have not been reported in previous articles. In addition, we investigated in detail the effects of loading method on the structural property of TiO_2/CFA, such as morphology, crystal structure, porous property and ultraviolet-visible absorption. At the same time, the photocatalytic activity and the recycling property of TiO_2/CFA were evaluated by the photocatalytic depigmentation and mineralization of methyl orange (MO) solution.

2. Experimental procedures

2.1. Materials

All the reagents used in this work were of analytical grade and were used without any further purification: methyl orange was purchased from the SSS Reagent Company, Ltd., Shanghai, China. All the other reagents, such as tetrabutyl titanate, acetic acid and absolute ethanol were purchased form Sinopharm Chemical Reagent Company, Ltd., China. Deionized water was used to prepare the solutions in our experiments. Titanium dioxide P25 was purchased from Degussa Corporation (76 wt% anatase and 24 wt% rutile, 99.8% purity). The CFA was obtained from thermal power plant of Songyu, Xiamen, China. Before using as substrate in our experiments, the CFA was calcined at 600 °C for 2 h in an air atmosphere (The obtaining CFA was mainly composed of quartz and mullite).

2.2. Preparation of TiO_2-coated coal fly ash

2.2.1. Sol–gel procedure

Before TiO_2 was loaded on CFA, TiO_2 sol had been prepared by sol–gel route as follows: tetrabutyl titanate (TEBT, 17.02 ml) and ethanol (30 ml) were mixed in a conical flask. A solution of ethanol (28.32 ml), deionized water (7.2 ml) and acetic acid (20 ml) was slowly added to the above mixture under agitation for 1 h at ambient temperature. The mixture was aged for 6 h at room temperature, and the transparent sol was obtained. Then, 10 g CFA was added into the above TiO_2 sol under vigorous stirring for 3 d. The final product was dried at 80 °C in an oven, finally, calcined at 600 °C for 2 h in air atmosphere. For convenience, the sample prepared by this procedure was labeled as TiO_2/CFA-1.

2.2.2. Ambient hydrolysis procedure

10 g CFA was added into a conical flask containing 17.02 ml TEBT under vigorous stirring. After agitating for 1 h, the mixture was poured on a flat and dry salver. The TEBT enwrapped on CFA was slowly hydrolyzed by adsorbing the vapor in ambient air. After finishing the hydrolysis reaction, the product was collected and calcined at 600 °C for 2 h in air atmosphere. For convenience, the sample prepared by this procedure was labeled as TiO_2/CFA-2.

2.2.3. Hybrid slurry procedure

10 g CFA was added into a conical flask containing 17.02 ml TEBT under vigorous stirring. After stirring for 1 h, 3.6 ml deionized water was added drop by drop into the mixture under agitation, then, hybrid slurry was obtained. The hybrid slurry was dried at 80 °C in an oven, finally, calcined at 600 °C for 2 h in air atmosphere. For convenience, the sample prepared by this procedure was labeled as TiO_2/CFA-3. In addition, a sample labeled as TiO_2/CFA-4 was prepared by the same method as TiO_2/CFA-3 except that 10 g CFA was changed into 5 g, which implied that TiO_2/CFA-4 was coated with a double amount of TiO_2 as compared to other TiO_2/CFA samples. (The theoretical TiO_2 contents of TiO_2/CFA-1, TiO_2/CFA-2 and TiO_2/CFA-3 anchored on 10 g CFA are 3.995 g, but for TiO_2/CFA-4, it is 3.995 g TiO_2 immobilized on 5 g CFA).

2.3. Preparation of TiO_2-uncoated coal fly ash

TiO_2-uncoated coal fly ash was also prepared for comparison. The TiO_2 sol prepared by sol–gel route was aged for 6 h at 60 °C, and then was dried at 80 °C in an oven. After that, it was milled to powder by a ceramic mortar. Then, the powder sample was calcined at 600 °C for 2 h in air atmosphere. We sign the sample prepared by this procedure as Ti600 in current work.

2.4. Characterizations

The morphologies of samples were observed by scanning electron microscope (SEM, JEM-7500, Japan). X-ray diffraction (XRD) patterns of all samples were obtained at room temperature with a diffractometer (X'pert PROMPD, Holand) with copper K_{al} radiation. The nitrogen adsorption–desorption isotherms, pore size distributions and specific surface areas were measured at 77 K using a micromeritics (Tristar 3000, America). Ultraviolet-visible (UV–vis) absorption spectroscopies of all samples were recorded by a Shimadzu spectrophotometer (UV-2450, Japan) equipped with an integrating sphere. The baseline correction was done using a calibrated sample of barium sulfate.

2.5. Photo reactor system and experimental procedures

The process of photo reaction was carried out in a photo reaction system. A 500-W medium-pressure mercury lamp with major emission at 365 nm, positioned in the center of a water-cooled quartz jacket, was used to offer ultraviolet irradiation. At the side of quartz jacket, a 50-ml cylindrical glass vessel was used as the reactive bottle to load reaction solution. The distance between mercury lamp and reactive bottle is 40 mm. In the bottom of the reactive bottle, a magnetic stirrer was equipped to achieve effective dispersion. Air was bubbled through the reaction solution from the bottom of the reactive bottle to ensure a constant dissolved oxygen concentration. The temperature of the reaction solution was maintained at 30 ± 0.5 °C by water-cooling. The initial concentration of MO was 20 mg l^{-1} and the initial volume of MO was 50 ml. At the given time intervals, 2 ml of samples were taken from the suspension and immediately centrifuged at 4000 rpm for 30 min to eliminate the solid particles. The filtrate was stored in the dark for needed analysis.

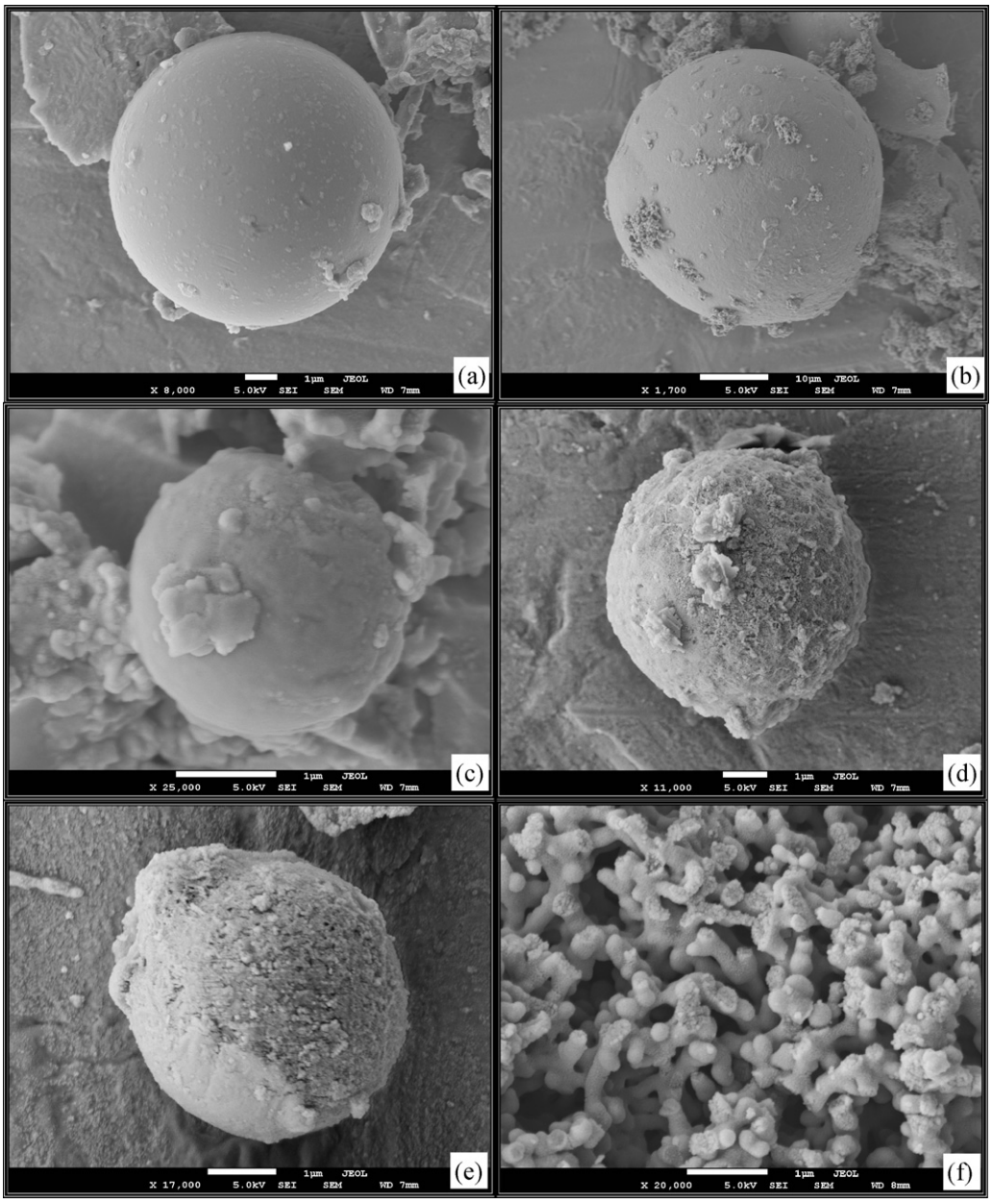

Fig. 1. SEM images of CFA and TiO_2/CFA samples: (a) CFA; (b) TiO_2/CFA-1; (c) TiO_2/CFA-2; (d) TiO_2/CFA-3; (e) and (f) TiO_2/CFA-4.

2.6. Reuse of the photocatalyst

Recycle experiment on photocatalytic decomposing of MO by TiO_2/CFA was designed to examine the recycling property of TiO_2/CFA. After finishing a cycle, the catalyst particles were precipitated in a quiescent condition for 60 min. Then the clear solution was removed from the reactive bottle and 50 ml fresh MO solution (initial concentration is 20 mg l^{-1}) was injected into the reactive bottle, and then the next cycle began. Each cycle lasted 40 min under ultraviolet irradiation. The recycle experiment was carried out for six cycles.

2.7. Analytic method

To measure MO concentration, a spectrophotometer (SpectraMax M5) was used to determine the absorbance of MO at the wavelength of 465 nm. The total organic carbon (TOC) concentration was determined using a Total Organic Analyzer instrument (Shimadzu TOC-V CPH, Japan).

3. Experimental results and discussion

3.1. Morphology of samples

The SEM images of CFA and TiO_2-coated CFA are illustrated in Fig. 1. It can be observed from Fig. 1a that CFA is composed of smooth sphere and agglomerates, which are result from the cooling of molten products of the combustion of clay compounds in the original coal [43]. From Fig. 1b, it can be found that only a small part of TiO_2 is anchored on the surface of sphere, most of TiO_2 are congregated into many agglomerates and dispersed away from CFA sphere, which indicates that it is difficult to load TiO_2 on the surface of CFA by sol–gel procedure. Fig. 1c shows that the CFA sphere is totally covered by TiO_2 film, and the surface of TiO_2 film is very

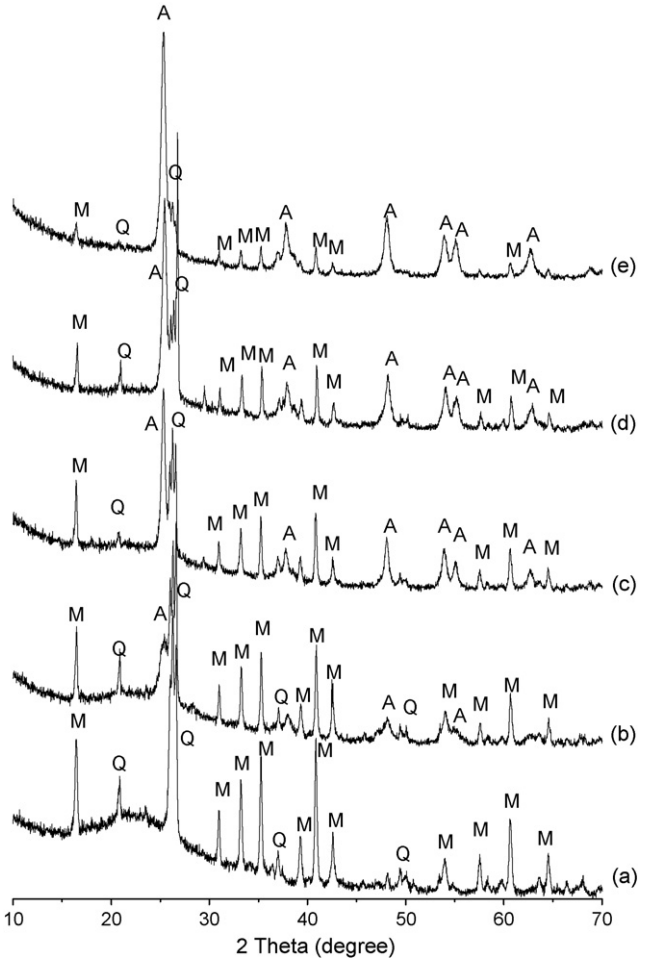

Fig. 2. XRD patterns of CFA and TiO_2/CFA samples (M: mullite; Q: quartz; A: anatase): (a) CFA; (b) TiO_2/CFA-1; (c) TiO_2/CFA-2; (d) TiO_2/CFA-3; (e) TiO_2/CFA-4 (M: mullite; Q: quartz; A: anatase).

smooth, which may be attributed to two facts that CFA is easy to be enwrapped by TEBT because of the glutinous property of TEBT, and the hydrolyzation of TEBT may be more uniform by adsorbing the vapor in ambient air. Fig. 1d shows that TiO_2 is loaded on CFA by the hybrid slurry procedure, but the surface of TiO_2 layer is very rough, which is unlike the sample prepared by the ambient hydrolysis procedure. The coating layer of TiO_2 loaded on CFA shown in Fig. 1e is very similar with that shown in Fig. 1d, which is due to the fact that the two samples were prepared by the same procedure. However, it is interesting that a three-dimensional (3D) network structure appears in the TiO_2/CFA-4 sample shown in Fig. 1f, and it can be observed from the image that the 3D network structure is formed by the interlocking together of many club-shaped materials.

3.2. Crystal structure of samples

XRD patterns of CFA and TiO_2/CFA are illustrated in Fig. 2. The XRD pattern of CFA shows that CFA sample contains quartz and mullite in large amount [44]. It can be observed that TiO_2 anchored on CFA all present anatase structure. Comparing with CFA, the intensity of diffraction peaks correlated with quartz and mullite becomes weak in TiO_2/CFA samples, which implies that TiO_2 have been loaded on the surface of CFA. The peak appeared at $2\theta = 25.4$ is the 1 0 1 plane of anatase TiO_2 [38], which is stronger in TiO_2/CFA-4 sample than that in other TiO_2/CFA samples. The peak appeared at $2\theta = 26.08$ is the diffraction peak of quartz [44], which becomes very weak in TiO_2/CFA-4 sample. The reason may attribute to the fact that more anatase TiO_2 was immobilized on the surface of CFA in TiO_2/CFA-4 sample.

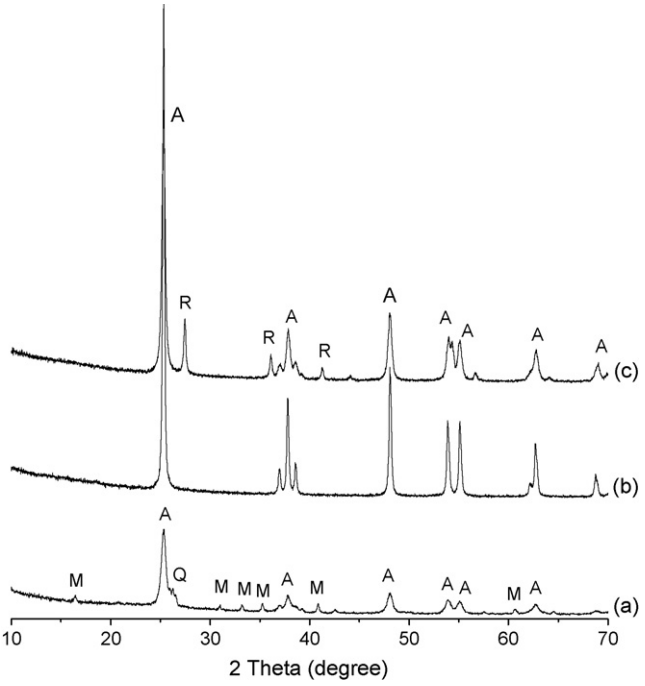

Fig. 3. XRD patterns of TiO_2/CFA-4 (a), Ti600 (b) and P25 (c): (M: mullite; Q: quartz; A: anatase; R: rutile).

Fig. 3 depicts the XRD patterns of TiO_2/CFA-4, Ti600 and P25 for comparison. It can be seen that TiO_2 existed in TiO_2/CFA-4 and Ti600 samples both present anatase phase, but some rutile structures appear in P25. Comparing with Ti600 sample, the diffraction peaks of anatase phase of TiO_2/CFA-4 sample become broader in width and weaker in intensity, which implies that CFA can inhibit the growth of nanocrystallite size of TiO_2. The result is also confirmed by the crystalline size of TiO_2 estimated from the (1 0 1) peak in the XRD pattern by applying the Scherrer formula [45,46] (The crystalline size of TiO_2 in Ti600, TiO_2/CFA-1, TiO_2/CFA-2, TiO_2/CFA-3, and TiO_2/CFA-4 is 51.9, 39.5, 47.4, 26.4 and 47.6 nm, respectively).

3.3. Nitrogen adsorption–desorption isotherm and porous property of samples

Fig. 4 shows the nitrogen adsorption–desorption isotherms of CFA and TiO_2/CFA samples. CFA and TiO_2/CFA-2 show an isotherm of type II (according to Brunauer's classification) and no hysteresis, referring to non-porous material [47]. While in case of TiO_2/CFA-1, TiO_2/CFA-3 and TiO_2/CFA-4, there is a hysteresis and almost matches a type IV isotherm, which is characteristic of mesoporous materials [48]. Moreover, it can be seen that all TiO_2/CFA samples have higher adsorption capacity than CFA, which increases in the order CFA < TiO_2/CFA-1 < TiO_2/CFA-2 < TiO_2/CFA-3 < TiO_2/CFA-4. The highest adsorption capacity of TiO_2/CFA-4 may be attributed to the rough surface of TiO_2 layer covered on ACF and the pores formed by the 3D network structure.

The pore size distributions of CFA and TiO_2/CFA samples are expressed in Fig. 5. The pore size distributions of TiO_2/CFA-3 and TiO_2/CFA-4 are very similar and have a sharp maximum at about 3.4 nm because of the same preparation procedure. Comparing with other samples, it can be concluded that many pores have been formed in the two samples, which indicate that the hybrid slurry procedure is a good method to synthesize TiO_2/CFA material with large specific surface area. The specific surface area of

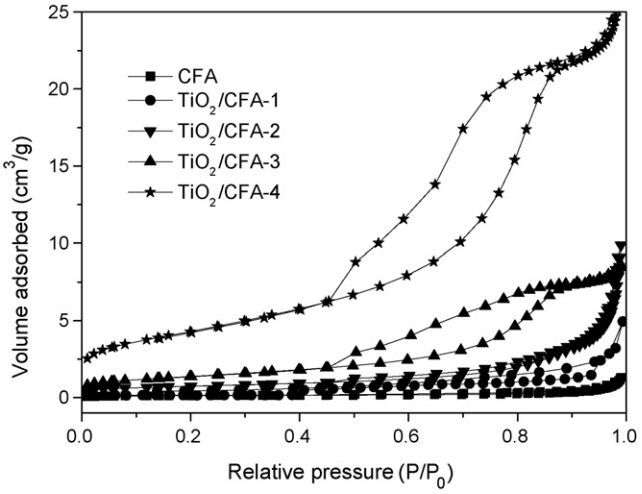

Fig. 4. Nitrogen adsorption–desorption isotherms of CFA and TiO_2/CFA samples.

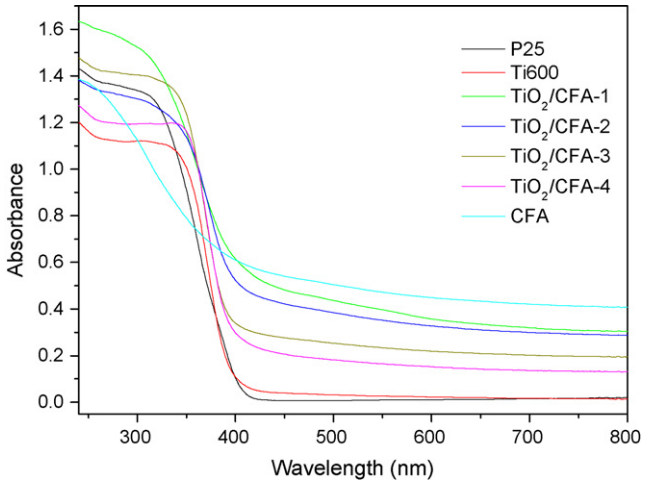

Fig. 6. UV–vis absorption spectroscopy of samples.

CFA, TiO_2/CFA-1, TiO_2/CFA-2, TiO_2/CFA-3, and TiO_2/CFA-4 is 0.4, 0.6, 2.5, 4.9 and 15.5 $m^2\ g^{-1}$, respectively, which is consistent with the adsorption capacity of samples deduced from Fig. 4.

3.4. UV–vis absorption spectroscopy of samples

Fig. 6 presents the UV–vis absorption spectroscopy of TiO_2/CFA samples, and CFA, Ti600 and P25 are also measured for comparison. It can be seen that CFA, with the color of gray, exhibits strong absorption in whole range of wavelength employed. All of the spectrums (except for CFA) clearly show the characteristic absorption edge of semiconductor TiO_2. Comparing with Ti600 and P25, the absorbances of TiO_2/CFA samples increase at the region of visible light starting at around 400 nm, and the absorption profiles of TiO_2/CFA samples shift to a longer wavelength region because of the impact of CFA.

3.5. Photocatalytic activity of samples

The photocatalytic activity of samples was measured by the depigmentation ratio of MO solution without concerning the degradation intermediates in detail, that is:

$$\eta_D(\%) = \frac{100(C_0 - C_t)}{C_0}(\%)$$

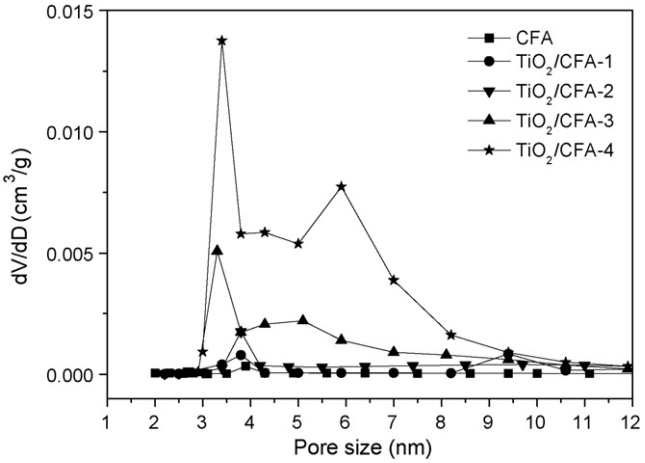

Fig. 5. Pore size distributions of CFA and TiO_2/CFA samples.

Where, η_D is the depigmentation ratio of MO solution, C_0 and C_t are the concentration of MO solution at the initial time and t time, respectively. For comparison, the photocatalytic activity of Ti600 and P25 was also tested. The added amount of sample is 0.3 g for CFA and TiO_2-coated CFA samples, and 0.1 g for Ti600 and P25, respectively, which are the optimal added amount for the two kinds of samples in our experimental condition. The depigmentation ratio of MO solution versus photocatalytic time under mercury lamp irradiation is shown in Fig. 7. It can be seen from blank test (no added powder) that MO molecules are very difficult to be decomposed under UV irradiation only. The depigmentation ratio of CFA is lowest among all samples because CFA has not photocatalytic activity in nature. The photocatalytic activity of TiO_2/CFA samples increases in the order TiO_2/CFA-1 < TiO_2/CFA-2 < TiO_2/CFA-3 < TiO_2/CFA-4, which is consistent with the specific surface area of samples. Ti600 and P25 have higher photocatalytic activity than TiO_2/CFA samples.

It is well known that the photocatalytic reaction occurs on the surface of the catalysts, and recombination of the photogenerated electron and hole is very fast, so interfacial charge carrier transfer is possible only when the donor or acceptor is pre-adsorbed before the photocatalytic reaction. The preliminary adsorption of the sub-

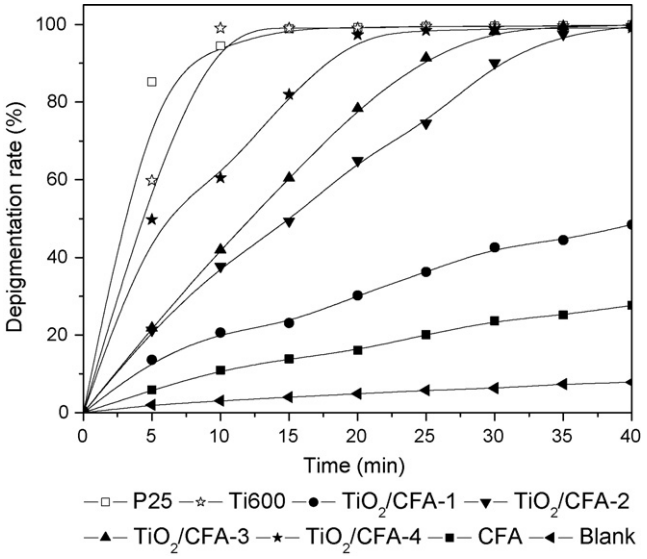

Fig. 7. Depigmentation ratio of MO solution versus photocatalytic time.

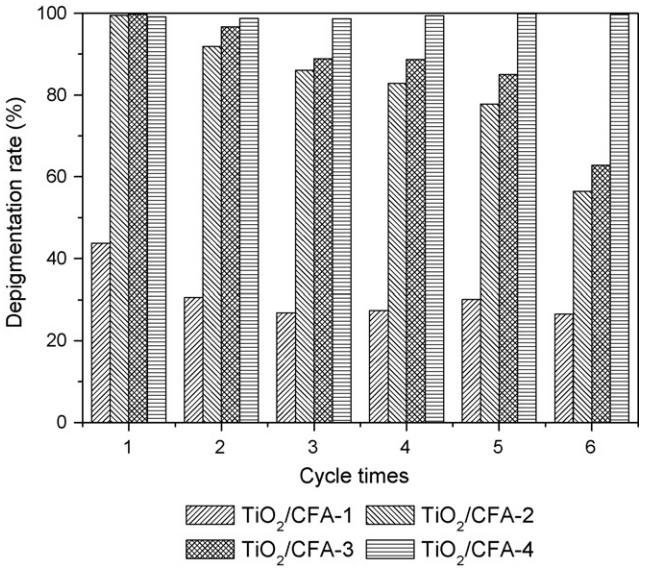

Fig. 8. Depigmentation ratio of MO solution versus cycle times.

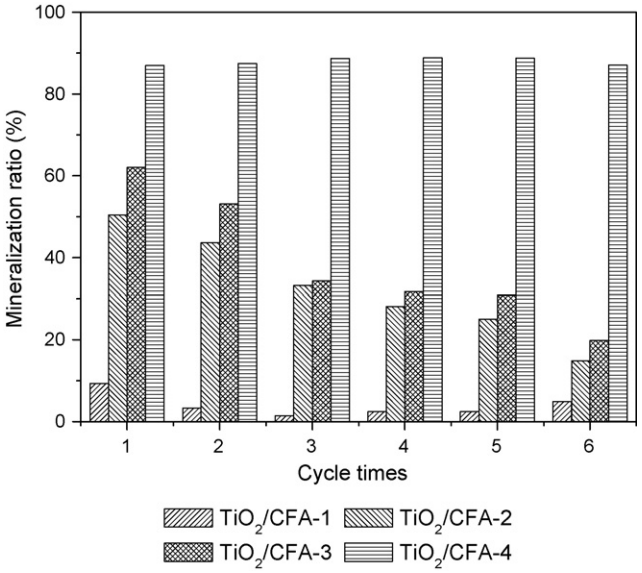

Fig. 9. Mineralization ratio of MO solution versus cycle times.

strates and the adsorption capacity of samples are very important pre-requisites for highly efficient degradation [49]. Larger specific surface area means more adsorption site. Samples with larger specific surface area can pre-adsorb more MO molecules on the surface of samples [50]. It may be the reason that the photocatalytic activity of TiO_2/CFA samples is positive correlation to the specific surface area of samples.

Comparing with TiO_2/CFA samples, TiO_2 powder samples (Ti600 and P25) are more effective to perform the depigmentation of MO solution. But the particle filtration after the decomposition increases the cost of this operation in industrial or large-scale applications. In addition, the cleaning and recycling of the powder catalyst are frequently impracticable due to the irreversible adsorption of some intermediate compounds, impregnation of organic matter and particles of substances used in the coagulation [51,52]. The use of TiO_2/CFA photocatalyst can be a remarkable alternative because the filtration step is not required. So it is worthy to improve the reused property of catalyst by sacrificing the photocatalytic activity in a certain extent.

Fig. 8 displays the depigmentation ratio of MO solution versus cycle times. It can be observed that the photocatalytic activity of TiO_2/CFA-1 is lowest among the four TiO_2/CFA samples from the first cycle to the sixth cycle, which may correlate with its smaller specific surface area and lower adsorption capacity. The photocatalytic activities of TiO_2/CFA-2 and TiO_2/CFA-3 are degressive with the increase of cycle times. Comparing with TiO_2/CFA-2, TiO_2/CFA-3 has a higher photocatalytic activity, which is due to its larger specific surface area. TiO_2/CFA-4 sample always keeps the highest photocatalytic activity from the first cycle to the sixth cycle, which may be attributed to its larger specific surface area, porous structure formed by the 3D network and more TiO_2 photocatalyst contained in its structure.

3.6. Mineralization of MO

The ultimate product of the photocatalytic degradation of organic pollutions can be CO_2, H_2O and relevant inorganic ions. In order to evaluate the extent of mineralization of MO, the TOC of MO solution was tested. Fig. 9 shows the mineralization ratio of MO degradation after 40 min under UV light irradiation with six times cycles. The mineralization ratio is calculated by using the formula as follows:

$$\eta_M(\%) = \frac{100(TOC_0 - TOC_t)}{TOC_0}(\%)$$

Where, η_M is the mineralization ratio of MO solution, TOC_0 and TOC_t are the TOC of MO solution at the initial time and t time, respectively. It can be seen that the mineralization ratio by using TiO_2/CFA-1 as photocatalyst is under 10% from the first cycle to the sixth cycle, indicating low photocatalytic activity of TiO_2/CFA-1 sample. The depigmentation ratio of MO reaches 99% at the first cycle when TiO_2/CFA-2 or TiO_2/CFA-3 is used as photocatalyst (see Fig. 8), but the mineralization ratio only arrives to 50.4 and 62.1, respectively. The mineralization ratio is lower than the depigmentation ratio, because the mineralization ratio is attributable to the TOC removal, while the depigmentation ratio for MO is attributable to the breakage of –N=N– in the molecules of MO [53]. The mineralization ratio decreases gradually with the increase of the cycle times, however, when TiO_2/CFA-4 sample is utilized to degrade MO, a high mineralization ratio (up to 88%) is always maintained from the first cycle to the sixth cycle.

4. Conclusions

TiO_2/CFA samples were prepared by three kinds of methods, sol–gel procedure, ambient hydrolysis procedure and hybrid slurry procedure, respectively. The photocatalyst TiO_2/CFA particles are easy to separate from the treated wastewater, which is very important for the practical applications of TiO_2 to water treatment. Therefore, TiO_2/CFA may be a promising material for application in the removal of organic pollutants from water in the future. From the above experimental results and discussion, it can be concluded that:

(1) The precipitation method is not unique approach to load TiO_2 on CFA. Ambient hydrolysis procedure and hybrid slurry procedure both are good choice and simple method to realize the immobilization of TiO_2 on CFA. The photocatalyst TiO_2/CFA particles prepared by ambient hydrolysis procedure have a smooth appearance. However, the surface of TiO_2 layer covered on the surface of CFA is very rough when hybrid slurry procedure was utilized, which is advantaged to its lager specific surface area. Comparing with the two preparation approaches, sol–gel pro-

cedure is a poor loading method because TiO_2 is difficult to be anchored on the surface of CFA by this procedure.

(2) The photocatalyst TiO_2/CFA particles are easy to separate from the treated wastewater by precipitating in a quiescent condition for some time because of the heavy weight of CFA (See Fig. S1 in the Supporting Information), which provides dependability for the recycling property of TiO_2/CFA.

(3) The photocatalyst TiO_2/CFA-4 prepared by hybrid slurry procedure presents the highest photocatalytic activity and the best recycling property among all TiO_2/CFA samples. When TiO_2/CFA-4 particles are used as photocatalyst, the high depigmentation ratio (near to 100%) and mineralization ratio (up to 88%) of MO solution are always maintained from the first cycle to the sixth cycle, which may attributed to its larger specific surface area, porous structure formed by the 3D network and more TiO_2 photocatalyst contained in its structure.

Acknowledgements

This work was supported by the Knowledge Innovation Program of the Chinese Academy of Sciences, and by the Program of the Chinese Academy of Sciences named “Study of New Style Photocatalytic Materials”.

Appendix A. Supplementary data

Supplementary data associated with this article can be found, in the online version, at doi:10.1016/j.molcata.2009.01.016.

References

[1] M. Matheswaran, T. Karunanithi, J. Hazard. Mater. 145 (2007) 154.
[2] J.C. Garcia, K. Takashima, J. Photoch. Photobio. A 155 (2003) 215.
[3] D. Mohan, P.K. Singh, G. Singh, K. Kumar, Ind. Eng. Chem. Res. 41 (2002) 3688.
[4] C. Zhu, L. Wang, L. Kong, X. Yang, L. Wang, S. Zheng, F. Chen, M. Feng, H. Zong, Chemosphere 41 (2000) 303.
[5] T.E. Doll, F.H. Frimmel, Water Res. 39 (2005) 403.
[6] C. Sahoo, A.K. Gupta, A. Pal, Dyes Pigments 66 (2005) 189.
[7] A.J. Schuler, H. Jang, Water Res. 41 (2007) 2163.
[8] B. Shi, G.Y. Li, Y.J. He, J. Am. Leather Chem. As. 97 (2002) 98.
[9] E. Ofir, Y. Oren, A. Adin, Desalination 204 (2007) 87.
[10] W. Gernjak, T. Krutzler, R. Bauer, J. Sol. Energ-t Asme 129 (2007) 53.
[11] M. Vautier, C. Guillard, J.-M. Herrmann, J. Catal. 201 (2001) 46.
[12] T. Sano, N. Negishi, K. Uchino, J. Tanaka, S. Matsuzawa, K. Takeuchi, J. Photoch. Photobio. A 160 (2003) 93.
[13] J. Chen, M. Liu, J. Zhang, X. Ying, L. Jin, J. Environ. Manage. 70 (2004) 43.
[14] F. Harrelkas, A. Paulo, M.M. Alves, L.E. Khadir, O. Zahraa, M.N. Pons, F.P. van der Zee, Chemosphere 72 (2008) 1816.
[15] G.H. Tian, H.G. Fu, L.Q. Jing, C.G. Tian, J. Hazard. Mater. 161 (2009) 1122.
[16] R. Asahi, T. Morikawa, T. Ohwaki, K. Aoki, Y. Taga, Science 293 (2001) 269.
[17] C.M. Ling, A.R. Mohamed, S. Bhatia, Chemosphere 57 (2004) 547.
[18] Y.V. Kolen'ko, B.R. Churagulov, M. Kunst, L. Mazerolles, C. Colbeau-Justin, Appl. Catal. B 54 (2004) 51.
[19] K. Chiang, T.M. Lim, L. Tsen, C.C. Lee, Appl. Catal. A 261 (2004) 225.
[20] H. Yamashita, Y. Ichihashi, M. Harada, G. Stewart, M.A. Fox, M. Anpo, J. Catal. 158 (1996) 97.
[21] I. Mazzarino, P. Piccinini, Chem. Eng. Sci. 54 (1999) 3107.
[22] J.W. Shi, J.T. Zheng, P. Wu, X.J. Ji, Catal. Commun. 9 (2008) 1846.
[23] P.F. Fu, Y. Luan, X.G. Dai, J. Mol. Catal. A 221 (2004) 81.
[24] S. Yamazaki, S. Matsunage, K. Hori, Water Res. 35 (2001) 1022.
[25] E.P. Reddy, L. Davydov, P. Smirniotis, Appl. Catal. B: Environ. 42 (2003) 1.
[26] J.M. Herrmann, J. Matos, J. Disdier, C. Guillard, J. Laine, S. Malato, J. Blanco, Catal. Today 54 (1999) 255.
[27] M. Nazir, J. Takasaki, H. Kumazawa, Chem. Eng. Comm. 190 (2003) 322.
[28] M.C. Lu, J.N. Chen, K.T. Chang, Chemosphere 38 (1999) 617.
[29] Y.H. Ao, J.J. Xu, D.G. Fu, X.W. Shen, C.W. Yuan, Colloid Surface A 312 (2008) 125.
[30] M.L. Huang, C.F. Xu, Z.B. Wu, Y.F. Huang, J.M. Lin, J.H. Wu, Dyes Pigments 77 (2008) 327.
[31] M.L. Li, M.X. Xu, Y. Li, T. Nonferr, Metal. Soc. 16 (2006) 257.
[32] P. Pucher, M. Benmami, R. Azouani, G. Krammer, K. Chhor, J.-F. Bocquet, A.V. Kanaev, Appl. Catal. A 332 (2007) 297.
[33] E. Carpio, P. Zuniga, S. Ponce, J. Solis, J. Rodriguez, W. Estrada, J. Mol. Catal. A 228 (2005) 293.
[34] X. Zhang, L. Lei, J. Hazard. Mater. 153 (2008) 827.
[35] H. Cho, D. Oh, K. Kim, J. Hazard. Mater. 127 (2005) 187.
[36] V. HeÂquet, P. Ricou, I. Lecuyer, P. Le Cloirec, Fuel 80 (2001) 851.
[37] S.B. Wang, Y. Boyjoo, A. Chouei, Chemosphere 60 (2005) 1401.
[38] Y.T. Yu, Powder Technol. 146 (2004) 154.
[39] D.Y. Shin, K.N. Kim, S.M. Han, Mater. Sci. Forum 439 (2003) 308.
[40] I. Piwoński, Thin Solid Films 515 (2007) 3499.
[41] S. Horikoshi, N. Watanabe, H. Onishi, H. Hidaka, N. Serpone, Appl. Catal. B 37 (2002) 117.
[42] S. Gelover, P. Mondragon, A. Jimenez, J. Photochem. Photobiol. A 165 (2004) 241.
[43] C.D. Woolard, J. Strong, C.R. Erasmus, Appl. Geochem. 17 (2002) 1159.
[44] Y.C. Dong, X.Q. Liu, Q.L. Ma, G. Meng, J. Membrane Sci. 285 (2006) 173.
[45] R. Vinu, G. Madras, J. Mol. Catal. A 291 (2008) 5.
[46] X. Fan, X. Chen, S. Zhu, Z. Li, T. Yu, J. Ye, Z. Zou, J. Mol. Catal. A 284 (2008) 155.
[47] T. Lopez, F. Rojas, R. Alexander-Katz, F. Galindo, A. Balankin, A. Buljan, Porosity, J. Solid State Chem. 177 (2004) 1873.
[48] Y. Liu, Y. Li, Y.T. Wang, L. Xie, J. Zheng, X.G. Li, J. Hazard. Mater. 150 (2008) 153.
[49] A.W. Xu, Y. Gao, H.Q. Liu, J. Catal. 207 (2002) 151.
[50] J.W. Shi, J.T. Zheng, P. Wu, J. Hazard. Mater. 161 (2009) 416.
[51] H. Choi, E. Stathatos, D.D. Dionysiou, Appl. Catal. B 63 (2006) 60.
[52] S. Gelover, P. Mondragón, A. Jiménez, J. Photochem. Photobiol. A 165 (2004) 241.
[53] C.H. Liang, C.S. Liu, F.B. Li, F. Wu, Chem. Eng. J. 147 (2009) 219.